JCI insight

RESEARCH ARTICLE

1,25-Dihydroxyvitamin D suppresses M1 macrophages and promotes M2 differentiation at bone injury sites

Samiksha Wasnik,[1] Charles H. Rundle,[2] David J. Baylink,[1] Mohammad Safaie Yazdi,[1] Edmundo E. Carreon,[1] Yi Xu,[1] Xuezhong Qin,[1,2] Kin-Hing William Lau,[1,2] and Xiaolei Tang[1]

[1]Division of Regenerative Medicine, Department of Medicine, Loma Linda University, Loma Linda, California, USA.
[2]Musculoskeletal Disease Center, Jerry L. Pettis Memorial VA Medical Center, Loma Linda, California, USA.

An indispensable role of macrophages in bone repair has been well recognized. Previous data have demonstrated the copresence of M1 macrophages and mesenchymal stem cells (MSCs) during the proinflammatory stage of bone repair. However, the exact role of M1 macrophages in MSC function and bone repair is unknown. This study aimed to define the role of M1 macrophages at bone injury sites via the function of 1,25-Dihydroxyvitamin D ($1,25[OH]_2D$) in suppressing M1 but promoting M2 differentiation. We showed that $1,25(OH)_2D$ suppressed M1 macrophage–mediated enhancement of MSC migration. Additionally, $1,25(OH)_2D$ inhibited M1 macrophage secretion of osteogenic proteins (i.e., Oncostatin M, TNF-α, and IL-6). Importantly, the $1,25(OH)_2D$-mediated suppression of osteogenic function in M1 macrophages at the proinflammatory stage was associated with $1,25(OH)_2D$-mediated reduction of MSC abundance, compromised osteogenic potential of MSCs, and impairment of fracture repair. Furthermore, outside the proinflammatory stage, $1,25(OH)_2D$ treatment did not suppress fracture repair. Accordingly, our data support 2 conclusions: (a) M1 macrophages are important for the recruitment and osteogenic priming of MSCs and, hence, are necessary for fracture repair, and (b) under vitamin D–sufficient conditions, $1,25(OH)_2D$ treatment is unnecessary and can be detrimental if provided during the proinflammatory stage of fracture healing.

Introduction

Mechanistically, bone repair can be divided into proinflammatory and regenerative stages (1, 2). Previous studies have demonstrated that the injury-induced immune response at the proinflammatory stage is necessary for the repair to progress (2). Recently, it has been realized that 1 specific immune cell population (i.e., macrophage) is present at all stages of fracture repair (3, 4). The importance of macrophages is well recognized because depletion of macrophages impairs bone repair (5, 6).

At least 2 subsets of macrophages have been reported. One macrophage subset is M1 macrophages, which are proinflammatory and secrete proinflammatory cytokines (e.g., TNF-α, IL-1α, IL-1β, IL-12, iNOS). The other macrophage subset is M2 macrophages, which are antiinflammatory and secrete anti-inflammatory cytokines (e.g., arginase 1 [ARG1], IL-10; ref. 7). Recent data have demonstrated that M1 macrophages are the dominant population of immune cells during the first 3 days of bone injury. These M1 macrophages are then gradually replaced by M2 macrophages. By day 7, the M2 macrophages become the dominant population of immune cells (8). To determine a potential temporal role of macrophages in bone repair, a recent study showed that a single injection of a macrophage depleting agent (i.e., clodronate-containing liposomes) before bone injury decreased the density and strength of newly formed bones by half. However, injection of the clodronate at days 1 and 3 after a bone injury yielded a statistically insignificant effect (9). Since it might take 2–3 days for the clodronate-containing liposomes to deplete macrophages at fracture sites, we reasoned that the delayed injections might not efficiently deplete M1 macrophages. Hence, the data appear to suggest that M1 but not M2 macrophages are critical for bone repair. The role of M1 macrophages in bone regeneration is also supported by the findings that M1 macrophages are known to synthesize Oncostatin M (OSM), TNF-α, and IL-6, which are osteogenic proteins necessary for normal bone repair (10–12). Additional evidence for the potential importance of M1 macrophages in bone repair

Conflict of interest: The authors have declared that no conflict of interest exists.

Submitted: November 20, 2017
Accepted: July 27, 2018
Published: September 6, 2018

Reference information:
JCI Insight. 2018;3(17):e98773.
https://doi.org/10.1172/jci.insight.98773.

is that M1, when compared with M2 macrophages, have been shown to more strongly enhance in vitro osteoblast differentiation in mesenchymal stem cells (MSCs) (13)

However, there are also reports suggesting otherwise. One report showed that switching from M1 to M2 at day 3 was necessary to further enhance the ability of macrophages to promote in vitro osteogenic differentiation (14). Additionally, an in vivo study demonstrated that an augmented differentiation of M2 macrophages at bone injury sites through a local single administration of collagen scaffold containing two M2 macrophage–differentiating cytokines (i.e., IL-4 and IL-13) promoted bone formation during the 3 weeks of investigation period (8). Although not dismissing the role of M1 macrophages, these data suggest a more important role for M2 macrophages during fracture repair (8).

To summarize, the exact role of M1 macrophages during bone repair is yet to be determined. In this regard, 1,25-Dihydroxyvitamin D ($1,25[OH]_2D$; i.e., the active vitamin D metabolite) has been shown to not only promote M2 macrophage differentiation, but also suppress M1 macrophage differentiation (15–17). Hence, knowledge on the effects of $1,25(OH)_2D$ treatment on the osteogenic function of M1 macrophages at fracture sites and on bone repair can shed light on the role of the 2 distinct macrophage subsets in bone repair. Additionally, knowing the effects of $1,25(OH)_2D$ treatment on bone repair is particularly important because there is an increasing interest in the supplementation of vitamin D for the prevention and treatment of various human diseases (e.g., multiple sclerosis, inflammatory bowel disease, and diabetes) due to an association of vitamin D deficiency with these diseases (18–21). More importantly, these diseases are frequently attended by an increasing risk of bone injuries (22–24).

In this study, we investigated the effects of $1,25(OH)_2D$ treatment on fracture healing, as well as on the interaction of macrophages with MSCs. Our goals were to perceive the role of M1 macrophages and $1,25(OH)_2D$ in bone repair in vitamin D–sufficient animals.

Results

$1,25(OH)_2D$ impaired fracture repair when s.c. administered locally at fracture sites during but not after the proinflammatory stage. To begin this study, we first investigated the effects of $1,25(OH)_2D$ treatment, beginning either at the proinflammatory stage or the regenerative stage, on fracture repair in vitamin D–sufficient animals. Accordingly, C57BL/6 (B6) mice were subjected to fracture surgery and received a daily s.c. dose of either vehicle control (VC) or 100 ng/kg $1,25(OH)_2D$ locally at fracture sites (Figure 1A). Radiographic analysis at days 0, 7, 14, 21, and 28 after the fracture surgery suggested that this early $1,25(OH)_2D$ treatment caused a delay in fracture repair (Figure 1B). Quantification of various parameters of fracture healing based on the radiographic images showed that this early $1,25(OH)_2D$ treatment reduced callus size by approximately 40% at day 14 (Figure1C, $P < 0.01$, $n = 5$). Additionally, bone union and cortex remodeling at day 28 showed approximately 65% and 50% reduction, respectively, as a result of the $1,25(OH)_2D$ treatment (25). Furthermore, H&E staining of the fractured bones showed that $1,25(OH)_2D$-treated fractures, when compared with VC-treated fractures, displayed bigger fracture gaps and fewer new bones at fracture sites (Figure 1D). To definitively determine whether the $1,25(OH)_2D$ treatment impaired fracture repair, we performed μCT analysis (Figures 1, E and F). Our data show that the bones spanning fracture sites of the animals receiving $1,25(OH)_2D$, when compared with VC, displayed approximately 25% reduction in the ratio of bone volume/total volume (BV/TV) and 5% reduction in trabecular thickness (Tb.Th) (Figure 1F, $P < 0.05$, $n = 5$). In contrast, the $1,25(OH)_2D$ treatment that started at day 10 after fracture did not significantly change fracture repair, although it did not significantly accelerate fracture repair, either (Supplemental Figure 1; supplemental material available online with this article; https://doi.org/10.1172/jci.insight.98773DS1).

Collectively, our data demonstrate that $1,25(OH)_2D$ treatment, under vitamin D–sufficient conditions, impairs normal fracture repair predominantly at proinflammatory but not regenerative stages.

$1,25(OH)_2D$ treatment at proinflammatory stage suppressed M1 differentiation but augmented M2 differentiation in macrophages at fracture sites. The foregoing findings demonstrate that $1,25(OH)_2D$ treatment, under vitamin D–sufficient conditions, suppresses bone repair mechanisms specifically at the proinflammatory stage. Additionally, we have learned from previous studies that a unique mechanism at the proinflammatory stage of bone repair is M1 macrophage differentiation and that $1,25(OH)_2D$ decreases M1 differentiation but increases M2 differentiation in macrophages (8, 17). These findings from our laboratory and others led us to reason that the early $1,25(OH)_2D$ treatment could potentially help address the unsettled importance of M1 and M2 macrophages in bone repair. Because previous data on the role of $1,25(OH)_2D$ in M1 and

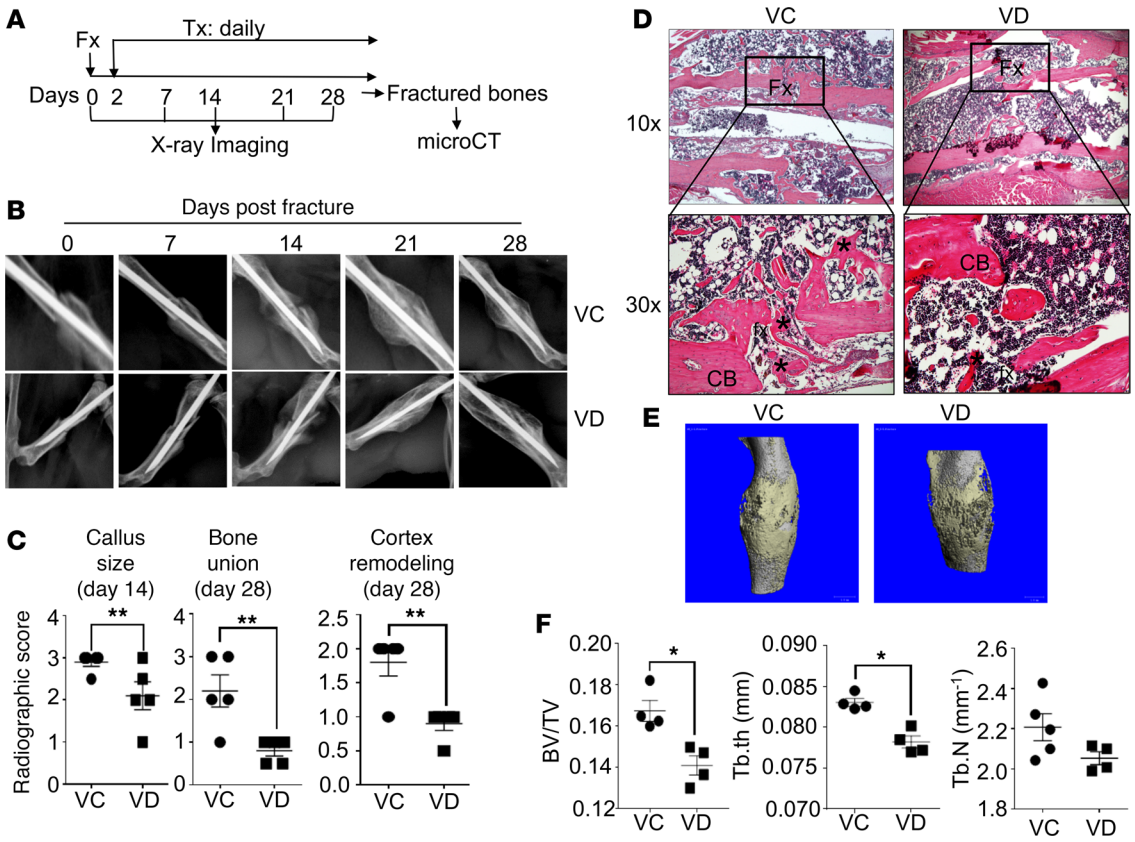

Figure 1. Local s.c. treatment with 1,25(OH)$_2$D during proinflammatory stage impaired fracture healing. (**A** and **B**) B6 mice were subjected to fracture surgery (Fx). Two days later, the animals received a daily s.c. dose of either vehicle control (VC) or 100 ng/kg 1,25(OH)$_2$D (VD) at fracture sites (Tx). X-ray images of the fractured bones were taken at days 0, 7, 14, 21, and 28. Additionally, at day 28, the fractured bones were collected from the animals for μCT analysis. Representative X-ray images are shown. (**C**) X-ray images from day 14 were quantified for callus size and those from day 28 for bone union and cortex remodeling. $^{**}P < 0.01$, *t* test, $n = 5$. (**D**) Representative images of H&E staining of the fractured bones are shown. Upper panels, 10×; lower panel:, 30×. Fx, fracture sites; CB, cortical bones; *, new bones. (**E**) Representative μCT 3-D images are shown. (**F**) Cumulative data show bone volume/total volume (BV/TV), trabecular thickness (Tb.th), and trabecular number (Tb.N) from the μCT analysis. $^{*}P < 0.05$, *t* test, $n = 5$.

M2 macrophage differentiations were reported in different experimental systems (26), we proceeded to determine whether, under the same condition, 1,25(OH)$_2$D also decreased M1 differentiation but increased M2 differentiation in macrophages. Accordingly, we treated a macrophage cell line (i.e., RAW 264.7 cells; ref. 27) with LPS and IFN-γ to induce M1 differentiation (28) in the presence of different 1,25(OH)$_2$D concentrations (Figure 2A). Fluorescence-activated cell sorting (FACS) analyses showed that the mean fluorescence intensities (MFIs) of IL-1β and IL-12 in the RAW 264.7 cells were increased by the LPS and IFN-γ treatment, indicating M1 differentiation of the RAW 264.7 cells (29, 30). Such M1 differentiation was significantly inhibited by the addition of 1,25(OH)$_2$D. Additionally, we also treated BM-derived primary macrophages with LPS and IFN-γ to induce M1 differentiation and with IL-4 to induce M2 differentiation in the presence of different 1,25(OH)$_2$D concentrations. The cells were then analyzed by FACS (Figure 2, B and C) and quantitative PCR (qPCR) (Figure 2D). Our data show that 1,25(OH)$_2$D significantly decreased the MFI of iNOS (an M1 macrophage marker) in the macrophages under the M1 differentiation condition but significantly increased the MFI of ARG1 (an M2 macrophage marker) in the macrophages under M2 differentiation conditions (Figure 2, B and C). qPCR analyses showed similar results (Figure 2D). In conclusion, our data clearly demonstrate that 1,25(OH)$_2$D suppresses M1 differentiation but enhances the M2 differentiation in macrophages in vitro.

However, whether the early 1,25(OH)$_2$D treatment, similar to our in vitro observations, suppresses M1 differentiation but augments M2 differentiation during bone repair was not previously studied. To address this question, B6 mice with femoral fracture surgery received a daily s.c. dose of either VC or 100 ng/kg/mouse 1,25(OH)$_2$D at fracture sites immediately after the fracture surgery (Supplemental Figure 2A). At days 1, 4, and 7, intact bones and bones spanning fracture sites (fractured bones) were analyzed

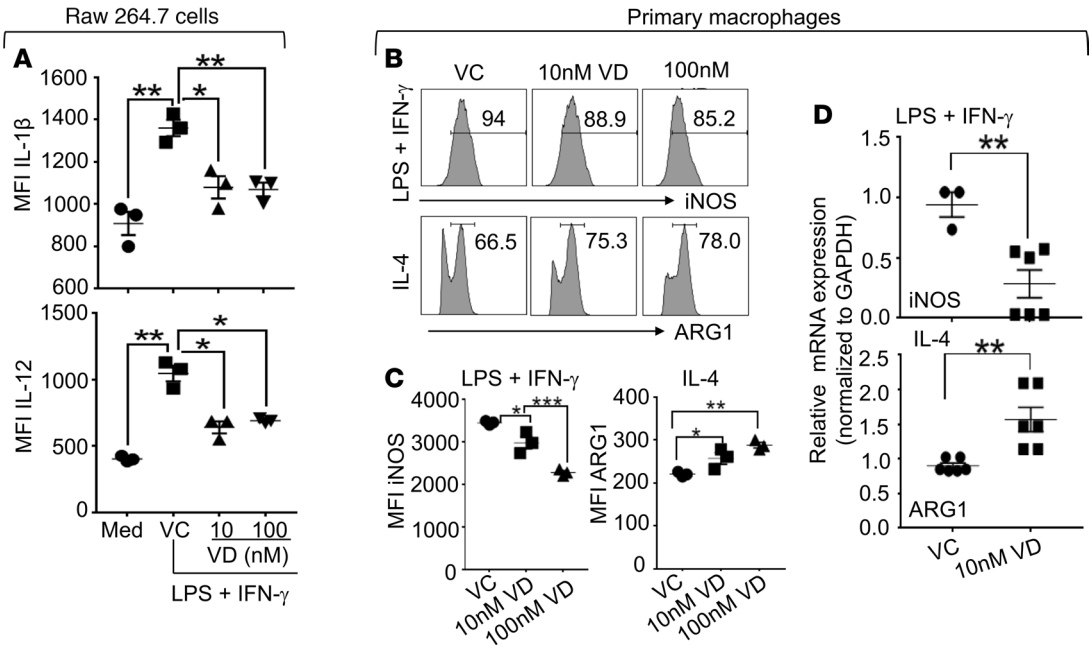

Figure 2. 1,25(OH)$_2$D suppressed M1 macrophage differentiation but augmented M2 macrophage differentiation in vitro. (**A**) RAW 264.7 cells were cultured in the absence or presence of LPS and IFN-γ. Additionally, the cultures that contained LPS and IFN-γ were added with vehicle control (VC), 10 nM 1,25(OH)$_2$D (VD), or 100 nM 1,25(OH)$_2$D (VD). Twenty-four hours later, the cells were stimulated with a cell-stimulation cocktail in the presence of a protein transport inhibitor cocktail overnight. The cells were then analyzed for the expressions of IL-1β and IL-12 by FACS. Data show the mean fluorescence intensities (MFIs) of IL-1β and IL-12. (**B–D**) Primary macrophages were generated from BM. The BM-derived primary macrophages were differentiated into M1 (LPS + IFN-γ) or M2 (IL-4) in the presence of VC, 10 nM 1,25(OH)$_2$D (VD), or 100 nM 1,25(OH)$_2$D (VD). Twenty-four hours later, the cells were stimulated as described in **A**. After the stimulation, the cells that cultured under the M1 differentiation conditions were analyzed for the expressions of iNOS, and those under the M2 differentiation conditions were analyzed for the expression of arginase 1 (ARG1) by FACS (**B** and **C**) and qPCR (**D**). Representative FACS plots are shown in **B**; MFIs of iNOS and ARG1 are shown in **C**; mRNA expressions of iNOS and ARG1 are shown in **D**. $^*P < 0.05$, $^{**}P < 0.01$, $^{***}P < 0.001$, 2-way ANOVA, $n = 3$.

by qPCR for the mRNA expressions of the markers for macrophages (i.e., F4/80 and CD11b) and for M1 macrophages (i.e., IL-1α and IL-1β). Data show that the bone injury significantly increased the mRNA expression levels of the marker genes for macrophages and M1 macrophages at days 1 and 4 at the fracture sites (Supplemental Figure 2, B and C). These increases of gene expressions in macrophages varied at day 7. The data suggest that M1-dominated immune response during a normal fracture healing process lasted for at least 4 days, a finding that was consistent with a recent analysis of macrophages at fracture sites showing that M1 macrophages dominated at days 1 and 3, and M2 macrophages dominated by day 7 (8). Importantly, our data show that the M1-dominated response appeared to be suppressed by the 1,25(OH)$_2$D treatment (Supplemental Figure 2, B and C).

However, one may argue that the changes observed in the qPCR analyses are not specific for macrophages because other cells can also express these markers. To address whether the observed changes in the expressions of CD11b, F4/80, IL-1α, and IL-1β indeed occurred in macrophages, we used FACS strategy to perform a further study. In this study, B6 mice with femoral fracture surgery s.c. received a daily dose of VC, 100 ng/kg/mouse 1,25 (OH)$_2$D, or 1,000 ng/kg/mouse 1,25(OH)$_2$D. At days 1, 4, and 7 after the treatments, cells were isolated from fracture sites and analyzed by FACS (Figure 3, A and B). Our data show that, at day 1, the MFIs of IL-1β and IL-12 were significantly increased in CD11b$^+$F4/80$^+$ macrophages during the proinflammatory stage of fracture healing (Figure 3, C and D), demonstrating an augmented differentiation of M1 macrophages (i.e., IL-1β^{hi} and IL-12^{hi} CD11b$^+$/F4/80$^+$ macrophages). Consistent with the increasing MFIs of IL-1β and IL-12, the percent of the IL-1β^{hi} and IL-12^{hi} macrophages was also significantly increased (Figure 3, C and E) at fracture sites when compared with the bones with no fracture. Additionally, the local s.c. treatment with 1,25(OH)$_2$D significantly reduced the MFIs of IL-1β and IL-12 in the viable CD11b$^+$F4/80$^+$ macrophages, as well as decreased the percent of IL-1β^{hi} and IL-12^{hi} CD11b$^+$F4/80$^+$ macrophages, confirming that the 1,25(OH)$_2$D treatment suppressed M1 macrophage differentiation. Similar to the qPCR observations, at days 4 and 7, the aforementioned changes subsided gradually (Supplemental Table 2).

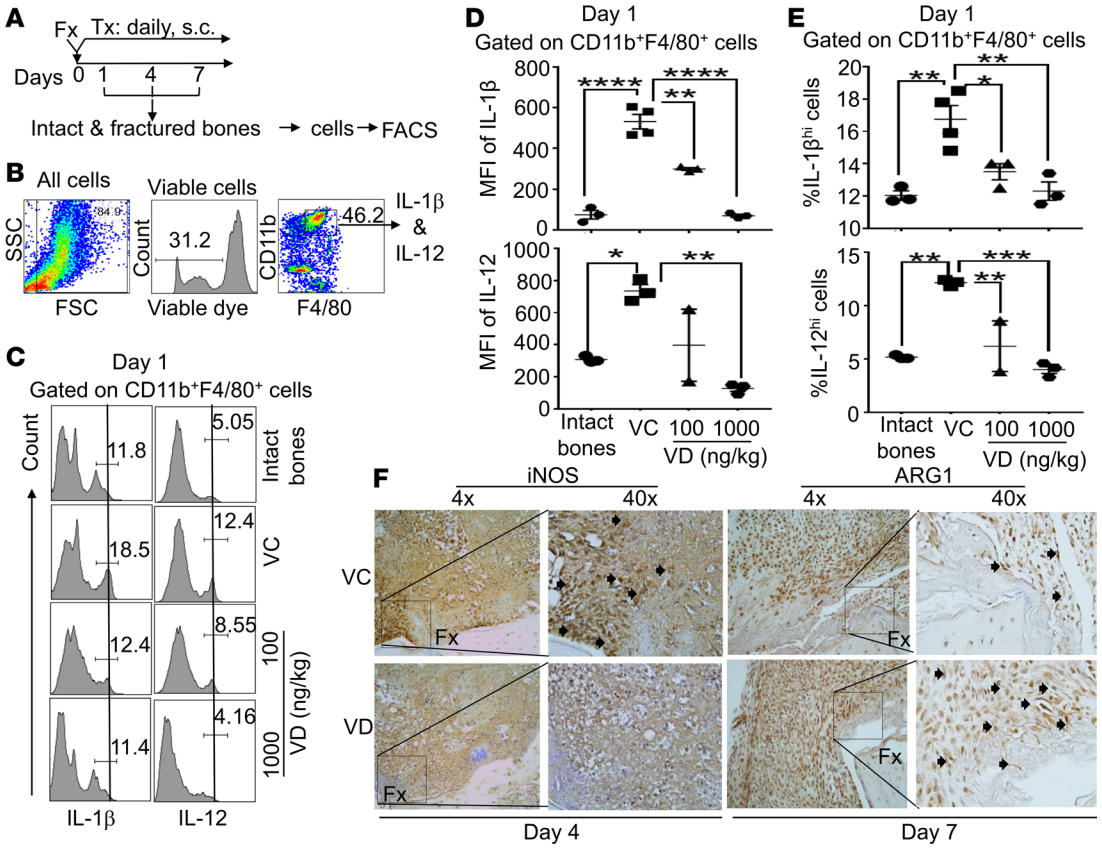

Figure 3. Local s.c. treatment with 1,25(OH)$_2$D at the proinflammatory stage suppressed M1 macrophage differentiation but augmented M2 macrophage differentiation at fracture sites. (**A**) B6 mice received femoral fracture surgery (Fx). Immediately after the fracture surgery, the animals received one of the following daily s.c. treatments (Tx) at fracture sites: a) vehicle control (VC), b) 100 ng/kg/mouse 1,25 (OH)$_2$D (VD), or c) 1,000 ng/kg/mouse 1,25(OH)$_2$D (VD). Additionally, a group of normal healthy mice was included as a control (intact bones). At days 1, 4, and 7 after the treatments, intact and fractured bones were collected, and cells were isolated as described in Methods. The cells were then analyzed by FACS. (**B**) Gating strategy shows that the cells are gated on viable CD11b$^+$/F4/80$^+$ macrophages for the FACS analysis. (**C**) Representative FACS plots show the expression of IL-1β (left panel) and IL-12 (right panel) in CD11b$^+$F4/80$^+$ macrophages at day 1 after the treatments. (**D**) Cumulative data of the mean fluorescent intensities (MFIs) of IL-1β (upper panels) and IL-12 (lower panels) expressions in CD11b$^+$F4/80$^+$ macrophages at day 1. (**E**) Cumulative data of the percent of IL-1β^{hi} and IL-12^{hi} cells among CD11b$^+$F4/80$^+$ macrophages at day 1. *P < 0.05, **P < 0.01, ***P < 0.001, ****P < 0.0001, ANOVA test, n = 3. (**F**) B6 mice were subjected to fracture surgery and, immediately after the fracture surgery, received a dose of either VC or 100 ng/kg 1,25(OH)$_2$D (VD). At days 4 and 7, fractured bones were collected. Paraffin embedded sections from day 4 were stained for iNOS and those from day 7 were stained for ARG1 by 3,3′-Diaminobenzidine (DAB) staining. Arrows indicate positively stained cells. Representative images are shown.

To further determine the effects of the 1,25(OH)$_2$D treatment on M1 and M2 differentiation, we analyzed the expression of iNOS and ARG1 at fracture sites by IHC. Our data show that the 1,25(OH)$_2$D treatment suppressed the expression of iNOS (an M1 macrophage marker) at day 4 after the treatment but augmented the expression of ARG1 (an M2 macrophage marker) at day 7 (Figure 3F).

Collectively, our data convincingly demonstrate that local s.c. treatment with 1,25(OH)$_2$D suppresses M1 differentiation but augments M2 differentiation in macrophages at the proinflammatory stage of bone repair. Additionally, our data also show that such local s.c. treatment with 1,25(OH)$_2$D produced similar effects in peripheral lymphoid tissues (i.e., spleens), but the effects were moderate (Supplemental Figure 3).

M1 macrophages enhanced MSC migration, which was suppressed by 1,25(OH)$_2$D. There are 2 important observations in our foregoing analyses of 1,25(OH)$_2$D treatment during fracture repair in vitamin D–sufficient animals: (a) the impairment of fracture repair only when 1,25(OH)$_2$D was administered in proinflammatory stage and (b) the suppression of M1 differentiation but augmentation of M2 differentiation when 1,25(OH)$_2$D was administered in the proinflammatory stage (Figures 1, 2, and 3). These observations suggest an irreplaceable role of M1 macrophages in bone repair. Since a central bone repair mechanism in the proinflammatory stage is the recruitment and osteogenic priming of MSCs, we investigated the potential role of M1 macrophages in this central repair mechanism. To address the role

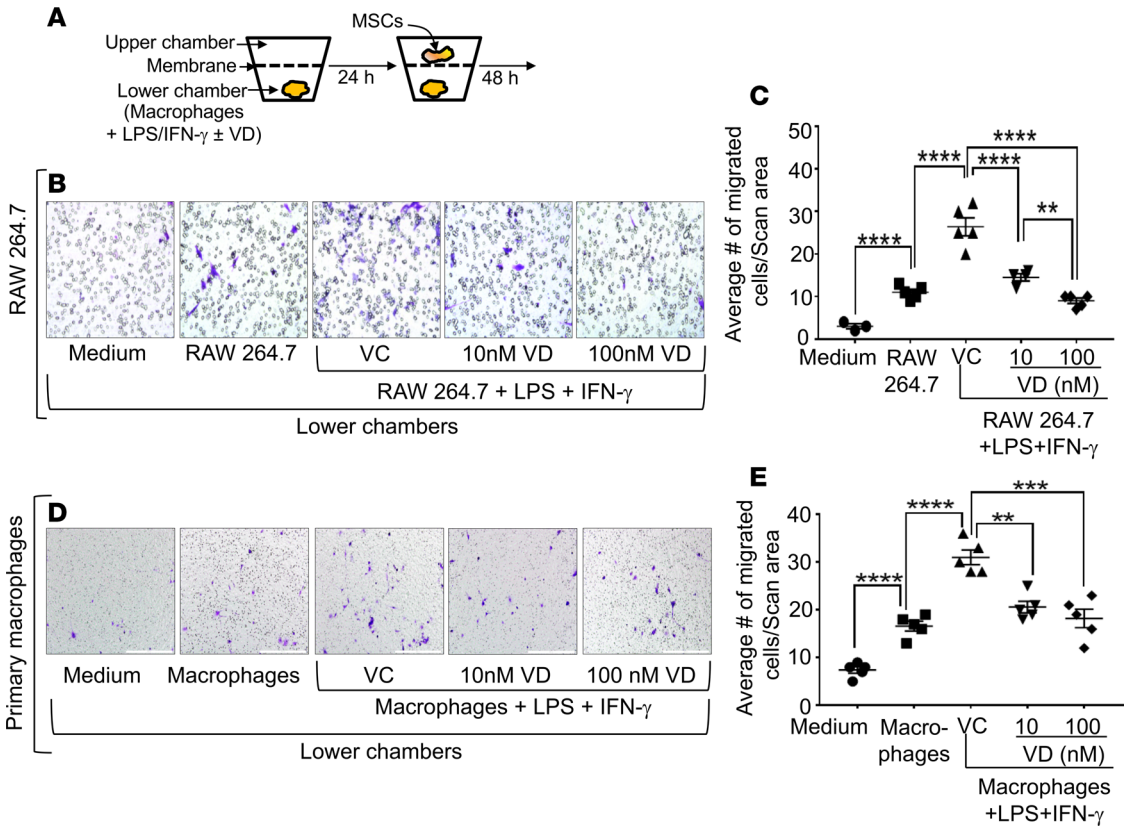

Figure 4. M1 macrophages enhanced the migration of MSCs, which was dose-dependently suppressed by 1,25(OH)$_2$D. (**A**) In a transwell culture system, the lower chambers were added with medium, RAW 264.7 cells, or RAW 264.7 cells + LPS + IFN-γ (M1 differentiation condition). Additionally, the wells, which contained RAW 264.7 cells + LPS + IFN-γ, were also added with vehicle control (VC), 10 nM 1,25(OH)$_2$D (10 nM VD), or 100 nM 1,25(OH)$_2$D (100 nM VD). Twenty-four hours later, BM-derived MSCs were added into upper chambers, and the cells were cultured. Twenty-four hours after that, the membranes were stained with crystal blue for the enumeration of migrated MSCs. (**B**) Representative microscopic images show the migration of MSCs in the membranes. Blue color indicates migrated cells. Magnification, 20×. (**C**) Cumulative data show migrated MSCs (average number of 3 different microscopic fields). (**D** and **E**) The same experiment was performed using BM-derived primary macrophages. Magnification, 10×. $^{**}P < 0.01$, $^{***}P < 0.001$, $^{****}P < 0.0001$, ANOVA, $n = 3$.

of M1 macrophages in MSC recruitment, as well as the potential impact of the 1,25(OH)$_2$D treatment, we cultured RAW 264.7 cells with BM MSCs in a transwell system under the M1 differentiation conditions as described in Figure 2 in the presence of different 1,25(OH)$_2$D concentrations (Figure 4A). Our data show that M1, when compared with undifferentiated RAW 264.7 cells, more strongly enhanced the migration of BM MSCs (Figure 4, B and C). Furthermore, this M1 macrophage–mediated enhancement of MSC migration was dose-dependently inhibited by 1,25(OH)$_2$D that was added during M1 differentiation of the RAW 264.7 cells. Additionally, we reproduced the above findings using BM-derived primary macrophages (Figure 4, D and E).

The observation that 1,25(OH)$_2$D suppresses M1-mediated enhancement of MSC migration suggests that the 1,25(OH)$_2$D treatment may reduce the abundance of MSCs at fracture sites during the proinflammatory stage. Indeed, our qPCR data show that the increasing mRNA expressions of the MSC marker genes (i.e., CD90, CD105, and CD73) at fracture sites at days 1 and 4 were significantly suppressed by the early 1,25(OH)$_2$D treatment (Supplemental Figure 4, A and B). Additionally, the 1,25(OH)$_2$D-mediated decrease in the expression of CD90 was also shown in our IHC analysis (Supplemental Figure 4C). To more precisely address the effects of the 1,25(OH)$_2$D treatment on MSCs, we performed FACS analysis. Our data further demonstrated that, following fracture surgery, the percentage of CD29$^+$, CD90$^+$, CD105$^+$, and CD73$^+$ MSCs was significantly increased among CD45$^-$ mesenchyme cells, which was suppressed by the 1,25(OH)$_2$D treatment (Figure 5 and Supplemental Table 3).

Collectively, we conclude that the early 1,25(OH)$_2$D treatment abrogates M1 macrophage–mediated enhancement of MSC recruitment, which is associated with a reduced abundance of MSCs at the proinflammatory stage of fracture healing.

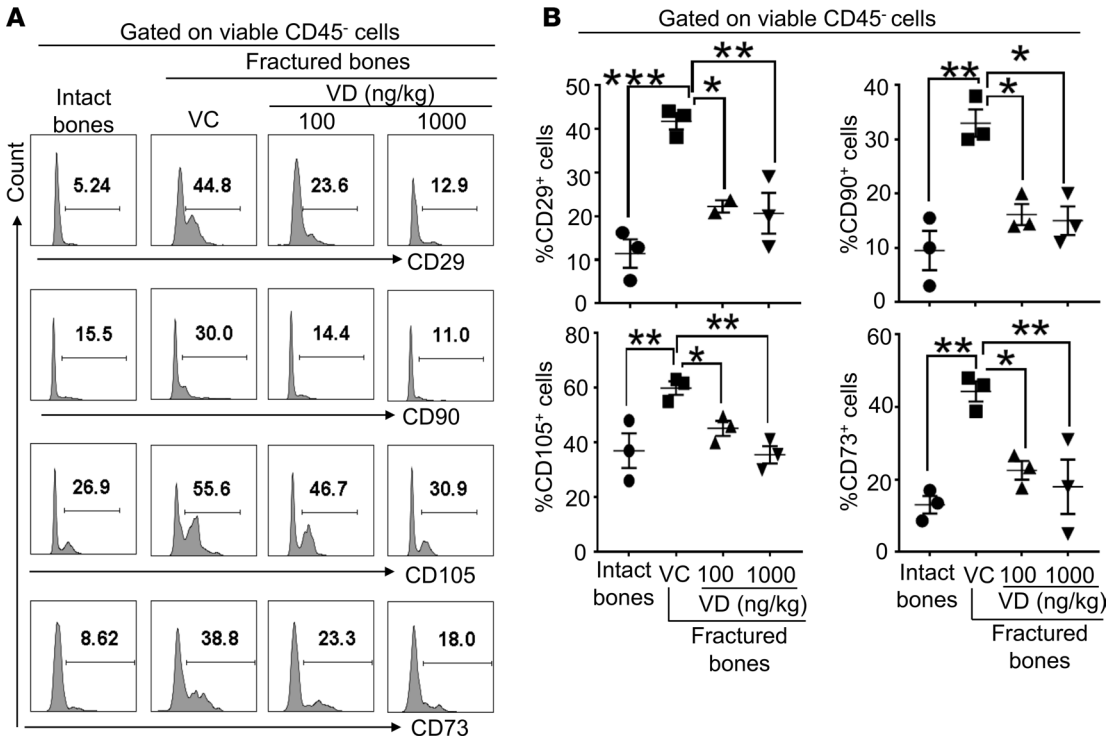

Figure 5. Local s.c. treatment with 1,25(OH)$_2$D during the proinflammatory stage reduced the abundance of CD29$^+$, CD90$^+$, CD105$^+$, and CD73$^+$ cells among CD45$^-$ mesenchyme cells at fracture sites. B6 mice were subjected to fracture surgery (Fx), treatments, cell isolation, and analyses as described in Figure 3. The cells from days 1, 4, and 7 were analyzed. Data from day 1 are shown. (**A**) Representative FACS histograms show the expressions of CD29, CD90, CD105, and CD73 in CD45$^-$ mesenchyme cells. (**B**) Cumulative data show the percent of CD29$^+$, CD90$^+$, CD105$^+$, and CD73$^+$ cells among CD45$^-$ mesenchyme cells. *P < 0.05, **P < 0.01, ***P < 0.001, ANOVA, n = 3.

M1 macrophages secreted high levels of osteogenic proteins at fracture sites, which was suppressed by 1,25(OH)$_2$D. In contrast to the scarce reports available on the role of macrophages in MSC recruitment, the role of macrophages in osteogenic differentiation of MSCs was intensively studied. Although the importance of M1 macrophage–associated molecules (i.e., OSM, TNF-α, and IL-6) for bone repair was convincingly demonstrated using animals deficient in these molecules (11, 31–33); data from other in vitro studies concerning the relative role of M1 and M2 macrophages in MSC osteogenic differentiation were not consistent (11–13, 34). We reasoned that this inconsistency of the data obtained from in vitro osteogenic differentiation assays might be caused by the experimental setup in which most designs added either M1 or M2 macrophages into a coculture system that lasted 3–4 weeks. However, in vivo, M1 macrophages were reprogrammed to M2 macrophages by day 7 (8). In light of this in vivo situation, a recent report demonstrated that switching of M1 macrophages to M2 macrophages beginning at day 3 was necessary to enhance in vitro osteogenic differentiation in MSCs (14), which appeared to resolve the inconsistency issue concerning the role of M1 macrophages in the augmentation of MSC osteogenic differentiation.

Based on these previous observations, we proceeded to determine the expression of OSM, TNF-α, and IL-6 at fracture sites and the effects of the early 1,25(OH)$_2$D treatment. Our data show that fracture significantly increased the mRNA expression of OSM, TNF-α, and IL-6 at days 1 and 7. Additionally, the early 1,25(OH)$_2$D treatment led to significant suppressions in the mRNA expressions of TNF-α and IL-6 at day 1 and of OSM and TNF-α at day 7. (Supplemental Figure 5, A and B). To further determine whether the increased production of OSM, TNF-α, and IL-6 indeed occurred in macrophages at fracture sites, we performed a FACS analysis. Our data show that fracture significantly increased the ability of macrophages to produce these 3 proteins, as manifested by the increasing MFIs of these proteins in macrophages (Figure 6, A and B) at day 1. Additionally, the increasing MFIs of the 3 proteins in macrophages were significantly suppressed by the early 1,25(OH)$_2$D treatment. Furthermore, the percent of OSM^{hi}, TNF-α^{hi}, and IL-6^{hi} cells were also increased at fracture sites at day 1. Again, the increasing percent of the OSM^{hi}, TNF-α^{hi}, and IL-6^{hi} cells in macrophages were significantly suppressed by the early 1,25(OH)$_2$D

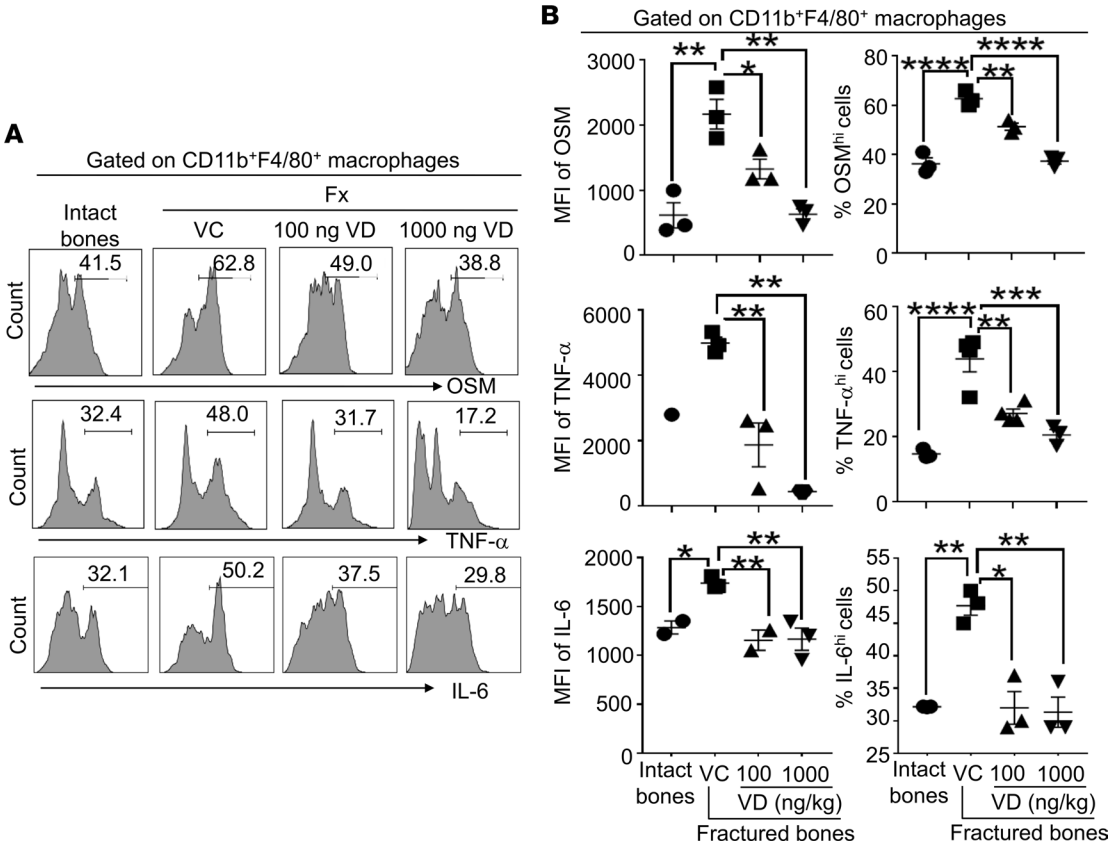

Figure 6. Local s.c. treatment with 1,25(OH)$_2$D during the proinflammatory stage suppressed at fracture sites CD11b$^+$F4/80$^+$ macrophage secretion of M1 macrophage–associated molecules that had been shown to promote osteogenesis in MSCs and to be important for fracture repair. B6 mice were subjected to fracture surgery (Fx), treatments, cell isolation, and analyses as described in Figure 3. The cells from days 1, 4, and 7 were analyzed. Data from day 1 are shown. (**A**) Representative FACS histograms show the expressions of Oncostatin M (OSM, upper panel), TNF-α (middle panel), and IL-6 (lower panel) in CD11b$^+$F4/80$^+$ macrophages. (**B**) Left, cumulative data of MFIs of OSM, TNF-α, and IL-6 expressions in CD11b$^+$F4/80$^+$ macrophages. Right, percent of OSM^{hi}, TNF-α^{hi}, and IL-6^{hi} cells among CD11b$^+$F4/80$^+$ macrophages. *P < 0.05, **P < 0.01, ***P < 0.001, ****P < 0.0001, ANOVA, n = 3.

treatment (Figure 6, A and B). Finally, these observed changes gradually subsided at days 4 and 7 following the fracture and the early 1,25(OH)$_2$D treatment (data not shown).

The observation that the local s.c. 1,25(OH)$_2$D treatment suppressed the production of OSM, TNF-α, and IL-6 in macrophages at fracture sites suggested that such treatment might compromise the ability of MSCs to differentiate into osteoblasts during fracture repair. To address this possibility, B6 mice were subjected to fracture surgery, 1,25(OH)$_2$D treatment, and analyses as described in Figure 3. Our data show that the fracture injury (VC), when compared with no fracture (intact bones), significantly increased the expression levels of the genes associated with osteoblast differentiation (i.e., runx2, osterix [OSX], and osteocalcin [OCN]) at the fracture sites at days 1 and 4 (Figure 7A). Additionally, the 1,25(OH)$_2$D treatment, when compared with the controls, significantly reduced the expression levels of runx2 and OCN.

To further determine whether the early 1,25(OH)$_2$D treatment reduced the osteogenic potential in MSCs at fracture sites, B6 mice were subjected to fracture surgery and 1,25(OH)$_2$D treatment as described in Figure 3. Four days later, CD45$^-$ mesenchyme cells were purified from the fracture calluses and analyzed in an in vitro bone nodule assay that is a classic method for evaluating osteogenic potential of MSCs (Figure 7B) (35). Our data show that the mesenchyme cells from the unmanipulated fracture sites, when compared with those from the intact bones, displayed much stronger mineralization (Figure 7, C and D, intact bones vs. VC). These data suggest that the fracture primed MSCs for osteogenic differentiation at fracture sites. Additionally, the mesenchyme cells from the fracture sites in the animals that were s.c. treated at fracture sites with 1,25(OH)$_2$D, when compared with those in the unmanipulated animals, displayed significantly decreased in vitro mineralization in a dose-dependent manner (Figure 7, C and D, VC vs. 100 ng/kg 1,25[OH]$_2$D vs. 1,000 ng/kg 1,25[OH]$_2$D).

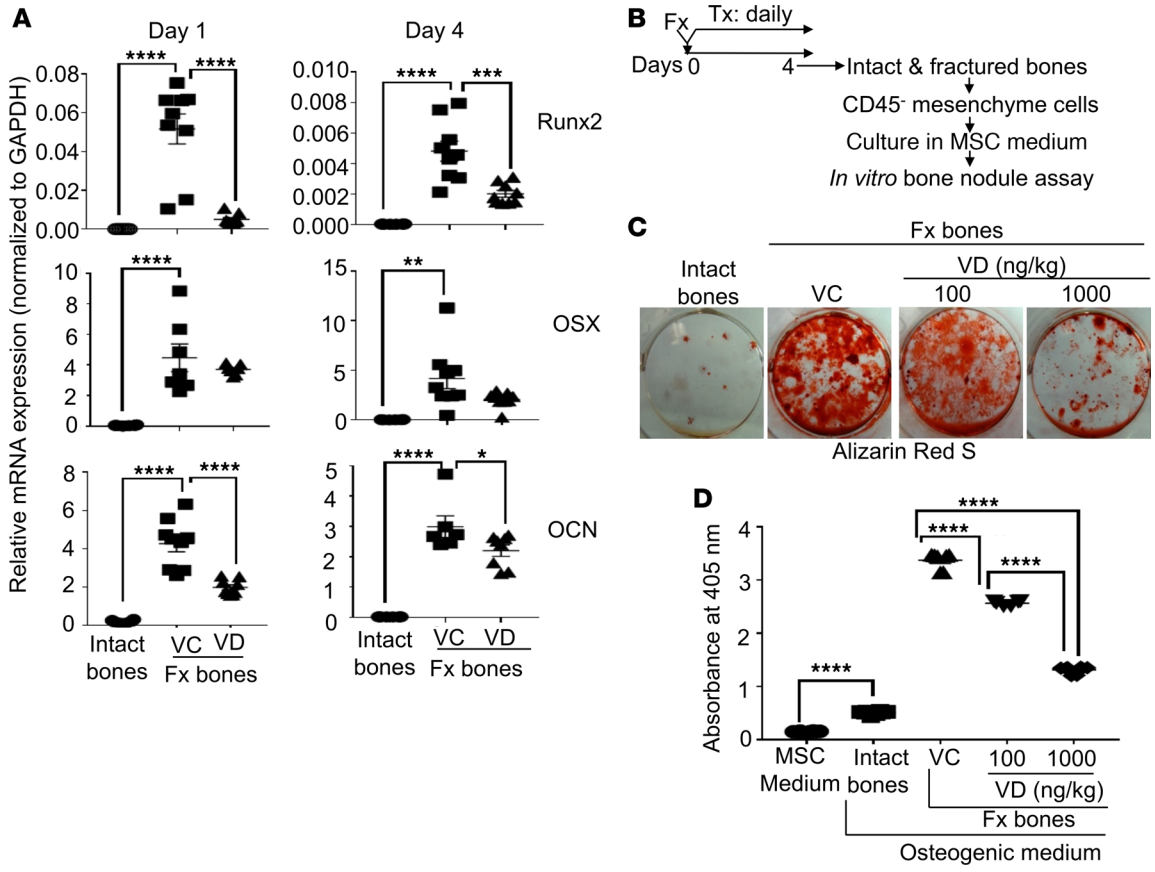

Figure 7. Local s.c. treatment with $1,25(OH)_2D$ during the proinflammatory stage compromised the osteogenic potential of MSCs at fracture sites. (**A**) B6 mice were subjected to fracture surgery (Fx). Immediately after the fracture surgery, the animals received a daily s.c. dose of either vehicle control (VC) or 100 ng/kg/mouse $1,25(OH)_2D$ (VD) at fracture sites. At days 1 and 4, intact (intact bones) and fractured (Fx bones) bones were examined for the mRNA expression of runx2, osterix (OSX), and osteocalcin (OCN) by qPCR. (**B**) B6 mice were subjected to fracture surgery. Immediately after the fracture surgery, the animals received a daily s.c. dose of VC, 100 ng/kg/mouse $1,25(OH)_2D$ (VD), or 1,000 ng/kg/mouse $1,25(OH)_2D$ (VD). At day 4, intact and fractured bones were collected for isolating $CD45^-$ mesenchyme cells. The purified cells were cultured in an MSC medium. Upon reaching 70%–80% confluence, an equal number of the cells were used for the in vitro bone nodule assay. (**C**) Representative images of Alizarin Red S staining at day 21 of the bone nodule assay. (**D**) Cumulative data of **C**. Where applicable, data are mean ± SEM. $^*P < 0.05$, $^{**}P < 0.01$, $^{***}P < 0.001$, $^{****}P < 0.0001$, ANOVA, n = (3-5).

Collectively, we conclude that the early $1,25(OH)_2D$ treatment inhibits the production of osteogenic proteins by M1 macrophages, which is associated with a compromised osteogenic potential in MSCs at the proinflammatory stage of fracture healing.

Discussion

Role of $1,25(OH)_2D$ in fracture repair. It has been well established that vitamin D is indispensable for bone healing because deficiencies in the production and function of $1,25(OH)_2D$ cause rickets (36, 37). Additionally, vitamin D deficiency causes nonunion fractures and pseudofractures, which can be very painful (38, 39), and treatment with vitamin D leads to a remarkable rescue of these mineralization defects. However, the animals used in our study were vitamin D sufficient. Analyses of $1,25(OH)_2D$ treatment at proinflammatory and regenerative stages of fracture repair demonstrated that a higher level of $1,25(OH)_2D$ at proinflammatory stage was detrimental to fracture repair and that a higher level of $1,25(OH)_2D$ at the regenerative stage did not further improve fracture repair. Hence, our findings support a conclusion that $1,25(OH)_2D$ treatment during fracture repair is unnecessary if patients are under vitamin D–sufficient conditions.

Mechanisms of $1,25(OH)_2D$-mediated suppression of fracture repair under vitamin D–sufficient conditions. With respect to the mechanisms by which the early $1,25(OH)_2D$ treatment reduces the osteogenic potential of MSCs at fracture sites and impairs fracture repair, we have now demonstrated that $1,25(OH)_2D$ does so by suppressing the osteogenic functions of M1 macrophages. Although this study does not

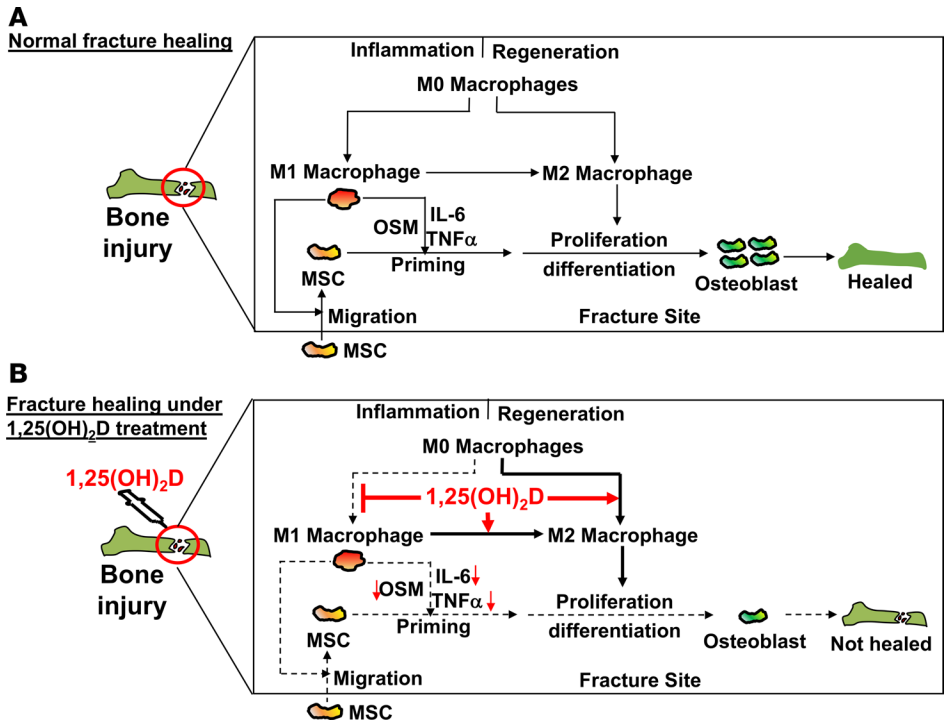

Figure 8. A model for the role of M1 macrophages and 1,25(OH)$_2$D treatment at the proinflammatory stage on bone repair under vitamin D–sufficient conditions.

exclude the possibility that 1,25(OH)$_2$D may act directly on MSCs at fracture sites, we reason that the early 1,25(OH)$_2$D treatment mainly acts on M1 macrophages because M1 macrophage differentiation is a currently known mechanism that is unique to the proinflammatory stage. Additionally, the following previous findings further corroborate our reasoning by demonstrating an irreplaceable role of M1 macrophages in bone repair. First, in animals where macrophages were depleted only at the proinflammatory stage, there was a severe impairment of fracture healing (9). Second, KO of M1 macrophage–derived cytokines (e.g., OSM, TNF-α, and IL-6) led to impaired fracture repair (11, 32, 33). Third, a deficiency of M1 macrophage–recruiting molecules (i.e., monocyte chemoattractant protein 1 receptor, also known as C-C motif chemokine receptor 2 [CCR-2]), led to compromised fracture healing (40). Fourth, cyclooxygenase 2 (COX-2) gene therapy accelerated fracture healing (41–43), and inhibitors of COX-2 compromised fracture healing primarily at the proinflammatory phase of fracture healing (44). This role of COX-2 in fracture repair is at least partially related to M1 macrophages because M1 macrophages depend on COX-2 to enhance in vitro osteoblast differentiation in MSCs (13). In aggregate, together with these previous reports, our current findings support the conclusion that M1 macrophages are indispensable for fracture repair, and vitamin D action to suppress fracture healing is mediated by the inhibition of M1 macrophages during the proinflammatory stage. This observation extends earlier work emphasizing the importance of a precisely coordinated immune system for fracture healing.

A model of 1,25 (OH)$_2$D-mediated impairment of fracture repair at proinflammatory stage under vitamin D–sufficient conditions. Based on our experimental results, we propose a model on normal fracture healing and the outcome of 1,25(OH)$_2$D treatment at the proinflammatory stage under vitamin D–sufficient conditions (Figure 8). In this model, bone injury first induces the differentiation of M1 macrophages that subsequently transdifferentiate into M2 macrophages at fracture sites (Figure 8A). The M1 macrophages promote the recruitment of MSCs, which increases the abundance of MSCs. In addition, the M1 macrophages also secrete osteogenic proteins (e.g., OSM, TNF-α, and IL-6) necessary for the osteogenic priming in MSCs, which leads to enhanced osteoblast differentiation. Ultimately, the fracture is healed. Treatment with 1,25(OH)$_2$D at the proinflammatory stage suppresses the osteogenic function in M1 macrophages (Figure 8B). Consequently, the recruitment and osteogenic priming of MSCs are also suppressed, which compromises osteoblast differentiation and, hence, impairs the healing of injured bones.

Role of 1,25(OH)$_2$D treatment under vitamin D–sufficient conditions in inflammation. Although our studies showed that the 1,25(OH)$_2$D-mediated inhibition of inflammation impaired fracture healing, a diametrically opposed result from a locally high-dose 1,25(OH)$_2$D treatment was found in experimental colitis (an animal model of human inflammatory bowel disease) and experimental allergic encephalomyelitis (an animal model of human multiple sclerosis) (45, 46). The different outcomes of the 1,25(OH)$_2$D treatment in these 2 distinct inflammatory conditions signify the importance of local tissue microenvironment for tissue repair (46, 47). Consistent with a recent review on inflammation (48), there are different types of inflammations. We extend this observation to show that 1,25(OH)$_2$D treatment is therapeutically beneficial for some inflammatory conditions but detrimental for others.

Limitation. A limitation of this study is that our data do not directly address the cause-and-effect relationship between the 1,25(OH)$_2$D-mediated suppression of osteogenic function in M1 macrophages and the 1,25(OH)$_2$D-mediated impairment of MSC osteogenic potential at fracture sites and fracture repair. Further investigations using conditional KO of vitamin D receptor (VDR) in M1 macrophages will help definitively determine this relationship.

Conclusion. This study aimed to perceive the importance of osteogenic function in M1 macrophages for osteoblast differentiation in MSCs at the proinflammatory stage and for fracture repair by way of the well-recognized 1,25(OH)$_2$D function in suppressing M1 but promoting M2 differentiation in macrophages. Our data from this study support 2 major conclusions: (a) M1 macrophages are important for the recruitment and osteogenic priming of MSCs during proinflammatory stage and, therefore, are indispensable for fracture repair, and (b) under vitamin D–sufficient conditions, 1,25(OH)$_2$D treatment during fracture repair is unnecessary and is even detrimental if provided during the proinflammatory stage of fracture healing.

Methods

Animals. Twelve-week-old male B6 mice were obtained from the Jackson Laboratory and housed in Loma Linda University Animal Care Facility.

Fracture surgery and X-ray imaging. A 30-gauge needle was inserted at a position just medial to the patella tendon into the BM cavity of a femur in a 12-week-old male B6 mouse. Fractures were created at the midshaft by a 3-point bending technique using an Instron Mechanical Tester, as described previously (42). Successful insertion of a needle and creation of fractures were confirmed by X-ray imaging in a Packard Faxitron X-Ray Digital Imaging equipment (25). X-ray images were taken at days 0, 7, 14, 21, and 28 following fracture surgery. Digital images were used for radiographic scorings. X-ray images at day 14 were used for the quantification of callus formation, and those at day 28 were used for quantification of bone union and callus remodeling (25).

1,25(OH)$_2$D treatments. Each animal received a daily s.c. treatment at fracture sites with either VC or 1,25(OH)$_2$ D (catalog 17936, MilliporeSigma). Two doses of 1,25(OH)$_2$D were used in this study (i.e., 100 ng/kg/mouse or 1,000 ng/kg/mouse). The injections were continued until the animals were euthanized.

μCT analysis. Femurs with fractures and intact femurs were harvested at day 28, fixed in 4% paraformaldehyde, and subjected to μCT analysis using a Scanco vivaCT μCT system with a voxel size of 10.5 μm. Mineralized callus bone was determined as previously described (49). Each sample was contoured around the periosteal circumference to determine the volume of interest (VOI) at a fracture site. The analysis thresholds were chosen to resolve the lower-density woven bone (220–570 mg/cm^3) from the higher-density native cortical bone (570–1,000 mg/cm^3) at fracture sites. The following parameters were reported in this study: BV/TV, Tb.th, and Tb.N (trabeculae number).

Isolation of mononuclear cells from fracture sites. Approximately 4 mm–length bones spanning fracture sites were harvested at different time points following fracture surgery, and the BM was flushed with sterile PBS (Invitrogen). The collected bones were digested with 2 mg/ml collagenase IV (Thermo Fisher Scientific) and 100 μg/ml DNase I (Roche Diagnostics) in PBS for 90 minutes at 37°C. Digested tissue samples were washed with PBS (600 g for 6 min at 4°C) and filtered through a 40-μm cell strainer. The digested suspensions were then washed with PBS and resuspended as single cell suspensions for downstream experiments.

In vitro bone nodule assay. To purify CD45$^-$ mesenchyme cells, the cells harvested from digested bone were stained with an anti–CD45-PE (catalog 553081, BD Pharmingen) followed by an anti–PE MicroBeads (catalog 130-048-801, Miltenyi Biotec). Subsequently, the MicroBeads-attached CD45$^+$ cells were removed by a magnet. The resulting CD45$^-$ mesenchyme cells were first cultured in an MSC medium (α-MEM medium containing 10% FBS [Invitrogen], 100 U/ml penicillin/streptomycin [Invitrogen], 3.125 × 10^{-5} M 2-ME [Thermo Fisher Scientific], 1 mM sodium pyruvate [Corning], 0.1 mM nonessential amino

acid [Invitrogen], and 2 mM L-glutamine [Invitrogen]). After reaching confluence, the $CD45^-$ mesenchyme cells were seeded in a 12-well tissue culture plate at an equal number per well in the presence or absence of an osteogenic medium (catalog CCM007, R&D Systems). At day 21, the cells were fixed in 4% formaldehyde, stained with Alizarin Red S (catalog TMS-008-C, MilliporeSigma), and imaged. To quantify calcium deposition, the Alizarin Red S–stained mineralized nodules were extracted with 10% (v/v) acetic acid, and an equal volume of the extracted solutions was transferred to a 96-well plate with transparent-bottom (Thermo Fisher Scientific). The plate was read at 405 nm on a microplate reader (BioTek Instruments Inc.) for the quantification of calcium deposition (50).

FACS analysis. FACS analysis was performed as described previously (46, 51). Briefly, cells at approximately 5×10^6 to 10×10^6 cells/ml were first incubated with anti-CD32 antibody (553141, BD Biosciences) at 4°C for 15 minutes to block Fc receptors before addition of fluorescence-labeled antibodies that stained cell surface proteins. The surface labeled cells were fixed with the intracellular fixation buffer (catalog 00-8222-49, eBioscience) followed by cell permeabilization (catalog 00-8333-56, eBioscience). The fixed and permeabilized cells were stained with fluorescence-labeled antibodies to stain intracellular proteins. The surface and intracellular-stained cells were washed, resuspended in FACS buffer (PBS, 1% FCS, 0.05% sodium azide), and analyzed in a FACS Aria II. The acquired data were analyzed using FlowJo software.

Antibodies used in this study include: anti-CD11b (557686, BD Biosciences), anti-F4/80 (123113, BioLegend), anti–IL-1β (clone NJTEN3, 12-7114-82, eBioscience), anti–IL-12 (clone C17.8, 12-7123-81, eBioscience), anti-OSM (AF-495-NA, RnD systems), anti–TNF-α (clone MP6 XT22, 12-7321-81, eBioscience), anti–IL-6 (11-7061-82, eBioscience), anti-CD45 (clone 30-f11, 552848, BD Biosciences), anti-CD29 (561796, BD Biosciences), anti-CD90 (553007, BD Biosciences), anti-CD105 (120416, BioLegend), and anti-CD73 (550741, BD Biosciences).

RNA isolation and qPCR analysis. Approximately 4 mm–long bones spanning fracture sites were excised and flash frozen in liquid nitrogen. Total RNA was isolated using the RNeasy Micro Kit (Qiagen) according to the manufacturer's instruction. First-strand cDNA was synthesized using the SuperScript III Reverse Transcriptase (Invitrogen; Life Technologies). qPCR was performed and analyzed in an Applied Biosystems 7900HT Real-Time PCR machine. Primers used in this study are listed in Supplemental Table 1. The PCR conditions were 10 minutes at 95°C followed by 40 cycles of 10 seconds at 95°C and 15 seconds at 60°C. The relative expression level of a gene was determined using ΔΔCt method and normalized to GAPDH (45).

MSC migration analysis. MSC migration assay was performed in a 24-well Corning Costar Transwell chamber using a porous polycarbonate membrane with a pore size of 8 μm (Thermo Fisher Scientific). Briefly, the lower chambers were seeded with 1 of the following components: (a) α-MEM medium (Med); (b) RAW264.7 cells or BM-derived primary macrophages; (c) RAW264.7 cells or BM-derived primary macrophages + 100 ng/ml LPS + 20 ng/ml IFN-γ + VC; (d) RAW264.7 cells or BM-derived primary macrophages + 100 ng/ml LPS + 20 ng/ml IFN-γ + 10 nM $1,25(OH)_2D$; or (e) RAW264.7 cells or BM-derived primary macrophages + 100 ng/ml LPS + 20 ng/ml IFN-γ + 100 nM $1,25(OH)_2D$. The cells were cultured at 37°C and 5% CO_2 for 24 hours to allow M1 differentiation. Subsequently, an equal number of MSCs in an MSC culture medium (α-MEM medium [Invitrogen] containing 10% FBS, 100 U/ml penicillin/streptomycin, 3.125×10^{-5} M 2-ME, 1 mM sodium pyruvate, 0.1 mM nonessential amino acid, and 2 mM L-glutamine) was seeded in the upper chambers. After 48 hours of coculture, the membranes were fixed in 4% formaldehyde and stained with 0.5% of crystal violet (MilliporeSigma). Numbers of migrated cells in the membrane in more than 3 randomly chosen microscopic fields were counted and averaged.

Statistics. All data were presented as mean ± SEM. Statistically significant differences were assessed by 1-way ANOVA or by independent unpaired parametric 2-tailed Student's *t* test. A *P* value of less than 0.05 was considered to be statistically significant.

Study approval. All in vivo animal study protocols were reviewed and approved by the Institutional Animal Care and Use Committee (IACUC) of Loma Linda University as well as the Animal Care and Use Review Office (ACURO) of the US Army Medical Research and Materiel Command (USAMRMC) of the Department of Defense.

Author contributions

SW, CHR, MSY, EEC, and YX performed the experiments. XT, DJB, XQ, and KHWL interpreted the data. XT and DJB conceived, directed, and supervised the study. XT, DJB, and SW wrote the manuscript. KHWL provided critical reading of the manuscript. All authors reviewed the manuscript.

Acknowledgments

We would like to thank Penelope Garcia of the Division of Regenerative Medicine of the Department of Medicine at the Loma Linda University for her technical assistance. This work was supported by the Telemedicine and Advanced Technology Research Center (TATRC) at the US Army Medical Research and Material Command (USAMRMC) under grant no. W81XWH-12-1-0023. The views, opinions, and/or findings contained in this report are those of the authors and should not be construed as an official Department of the Army position, policy, or decision unless so designated by other documentation.

Address correspondence to: Xiaolei Tang, Department of Medicine, Division of Regenerative Medicine, Loma Linda University, 11234 Anderson Street, Loma Linda, California 92354, USA. Phone: 909.651.5891; Email: Xitang@llu.edu.

1. Wang T, Zhang X, Bikle DD. Osteogenic Differentiation of Periosteal Cells During Fracture Healing. *J Cell Physiol*. 2017;232(5):913–921.
2. Loi F, Córdova LA, Pajarinen J, Lin TH, Yao Z, Goodman SB. Inflammation, fracture and bone repair. *Bone*. 2016;86:119–130.
3. Sinder BP, Pettit AR, McCauley LK. Macrophages: Their Emerging Roles in Bone. *J Bone Miner Res*. 2015;30(12):2140–2149.
4. Wu AC, Raggatt LJ, Alexander KA, Pettit AR. Unraveling macrophage contributions to bone repair. *Bonekey Rep*. 2013;2:373.
5. Vi L, et al. Macrophages promote osteoblastic differentiation in-vivo: implications in fracture repair and bone homeostasis. *J Bone Miner Res*. 2015;30(6):1090–1102.
6. Alexander KA, et al. Osteal macrophages promote in vivo intramembranous bone healing in a mouse tibial injury model. *J Bone Miner Res*. 2011;26(7):1517–1532.
7. Murray PJ. Macrophage Polarization. *Annu Rev Physiol*. 2017;79:541–566.
8. Schlundt C, et al. Macrophages in bone fracture healing: Their essential role in endochondral ossification. *Bone*. 2018;106:78–89.
9. Sandberg OH, Tätting L, Bernhardsson ME, Aspenberg P. Temporal role of macrophages in cancellous bone healing. *Bone*. 2017;101:129–133.
10. Glass GE, Chan JK, Freidin A, Feldmann M, Horwood NJ, Nanchahal J. TNF-alpha promotes fracture repair by augmenting the recruitment and differentiation of muscle-derived stromal cells. *Proc Natl Acad Sci USA*. 2011;108(4):1585–1590.
11. Guihard P, et al. Oncostatin m, an inflammatory cytokine produced by macrophages, supports intramembranous bone healing in a mouse model of tibia injury. *Am J Pathol*. 2015;185(3):765–775.
12. Guihard P, et al. Induction of osteogenesis in mesenchymal stem cells by activated monocytes/macrophages depends on oncostatin M signaling. *Stem Cells*. 2012;30(4):762–772.
13. Lu LY, et al. Pro-inflammatory M1 macrophages promote Osteogenesis by mesenchymal stem cells via the COX-2-prostaglandin E2 pathway. *J Orthop Res*. 2017;35(11):2378–2385.
14. Loi F, et al. The effects of immunomodulation by macrophage subsets on osteogenesis in vitro. *Stem Cell Res Ther*. 2016;7:15.
15. Zhang XL, Guo YF, Song ZX, Zhou M. Vitamin D prevents podocyte injury via regulation of macrophage M1/M2 phenotype in diabetic nephropathy rats. *Endocrinology*. 2014;155(12):4939–4950.
16. Wang F, Johnson RL, DeSmet ML, Snyder PW, Fairfax KC, Fleet JC. Vitamin D Receptor-Dependent Signaling Protects Mice From Dextran Sulfate Sodium-Induced Colitis. *Endocrinology*. 2017;158(6):1951–1963.
17. Han X, Li L, Yang J, King G, Xiao Z, Quarles LD. Counter-regulatory paracrine actions of FGF-23 and 1,25(OH)2 D in macrophages. *FEBS Lett*. 2016;590(1):53–67.
18. Al-Daghri NM, et al. Vitamin D Receptor Gene Polymorphisms Modify Cardiometabolic Response to Vitamin D Supplementation in T2DM Patients. *Sci Rep*. 2017;7(1):8280.
19. Mathur J, Naing S, Mills P, Limsui D. A randomized clinical trial of vitamin D3 (cholecalciferol) in ulcerative colitis patients with hypovitaminosis D3. *PeerJ*. 2017;5:e3654.
20. Miclea A, Miclea M, Pistor M, Hoepner A, Chan A, Hoepner R. Vitamin D supplementation differentially affects seasonal multiple sclerosis disease activity. *Brain Behav*. 2017;7(8):e00761.
21. Rejnmark L, et al. Non-skeletal health effects of vitamin D supplementation: A systematic review on findings from meta-analyses summarizing trial data. *PLoS One*. 2017;12(7):e0180512.
22. Briot K, Geusens P, Em Bultink I, Lems WF, Roux C. Inflammatory diseases and bone fragility. *Osteoporos Int*. 2017;28(12):3301–3314.
23. Dobson R, Ramagopalan S, Giovannoni G, Bazelier MT, de Vries F. Risk of fractures in patients with multiple sclerosis: a population-based cohort study. *Neurology*. 2012;79(18):1934–1935.
24. Lee RH, et al. Clinical Fractures Among Older Men With Diabetes Are Mediated by Diabetic Complications. *J Clin Endocrinol Metab*. 2018;103(1):281–287.
25. Chen L, et al. Platelet-rich plasma promotes healing of osteoporotic fractures. *Orthopedics*. 2013;36(6):e687–e694.
26. Zhang Y, et al. Vitamin D inhibits monocyte/macrophage proinflammatory cytokine production by targeting MAPK phosphatase-1. *J Immunol*. 2012;188(5):2127–2135.
27. Raschke WC, Baird S, Ralph P, Nakoinz I. Functional macrophage cell lines transformed by Abelson leukemia virus. *Cell*. 1978;15(1):261–267.
28. Ishizuka EK, et al. Role of interplay between IL-4 and IFN-γ in the in regulating M1 macrophage polarization induced by Nattectin. *Int Immunopharmacol*. 2012;14(4):513–522.
29. Gordon S. Alternative activation of macrophages. *Nat Rev Immunol*. 2003;3(1):23–35.
30. Krausgruber T, et al. IRF5 promotes inflammatory macrophage polarization and TH1-TH17 responses. *Nat Immunol*.

2011;12(3):231–238.
31. Wallace A, Cooney TE, Englund R, Lubahn JD. Effects of interleukin-6 ablation on fracture healing in mice. *J Orthop Res*. 2011;29(9):1437–1442.
32. Yang X, Ricciardi BF, Hernandez-Soria A, Shi Y, Pleshko Camacho N, Bostrom MP. Callus mineralization and maturation are delayed during fracture healing in interleukin-6 knockout mice. *Bone*. 2007;41(6):928–936.
33. Gerstenfeld LC, et al. Impaired fracture healing in the absence of TNF-alpha signaling: the role of TNF-alpha in endochondral cartilage resorption. *J Bone Miner Res*. 2003;18(9):1584–1592.
34. Zhang Y, Böse T, Unger RE, Jansen JA, Kirkpatrick CJ, van den Beucken JJJP. Macrophage type modulates osteogenic differentiation of adipose tissue MSCs. *Cell Tissue Res*. 2017;369(2):273–286.
35. Bellows CG, Aubin JE, Heersche JN, Antosz ME. Mineralized bone nodules formed in vitro from enzymatically released rat calvaria cell populations. *Calcif Tissue Int*. 1986;38(3):143–154.
36. Malloy PJ, Zhou Y, Wang J, Hiort O, Feldman D. Hereditary vitamin D-resistant rickets (HVDRR) owing to a heterozygous mutation in the vitamin D receptor. *J Bone Miner Res*. 2011;26(11):2710–2718.
37. Wang JT, et al. Genetics of vitamin D 1alpha-hydroxylase deficiency in 17 families. *Am J Hum Genet*. 1998;63(6):1694–1702.
38. Moore KR, Howell MA, Saltrick KR, Catanzariti AR. Risk Factors Associated With Nonunion After Elective Foot and Ankle Reconstruction: A Case-Control Study. *J Foot Ankle Surg*. 2017;56(3):457–462.
39. Lee C, Lashari S. Pseudofracture of the neck of femur secondary to osteomalacia. *J Bone Joint Surg Br*. 2007;89(7):956–958.
40. Xing Z, et al. Multiple roles for CCR2 during fracture healing. *Dis Model Mech*. 2010;3(7-8):451–458.
41. Lakhan R, et al. Local administration of AAV-DJ pseudoserotype expressing COX2 provided early onset of transgene expression and promoted bone fracture healing in mice. *Gene Ther*. 2015;22(9):721–728.
42. Lau KH, Kothari V, Das A, Zhang XB, Baylink DJ. Cellular and molecular mechanisms of accelerated fracture healing by COX2 gene therapy: studies in a mouse model of multiple fractures. *Bone*. 2013;53(2):369–381.
43. Rundle CH, et al. Retroviral-based gene therapy with cyclooxygenase-2 promotes the union of bony callus tissues and accelerates fracture healing in the rat. *J Gene Med*. 2008;10(3):229–241.
44. Giannoudis PV, Hak D, Sanders D, Donohoe E, Tosounidis T, Bahney C. Inflammation, Bone Healing, and Anti-Inflammatory Drugs: An Update. *J Orthop Trauma*. 2015;29 Suppl 12:S6–S9.
45. Liu H, et al. Local administration of calcitriol positively influences bone remodeling and maturation during restoration of mandibular bone defects in rats. *Mater Sci Eng C Mater Biol Appl*. 2015;49:14–24.
46. Li CH, et al. Dendritic cells, engineered to overexpress 25-hydroxyvitamin D 1α-hydroxylase and pulsed with a myelin antigen, provide myelin-specific suppression of ongoing experimental allergic encephalomyelitis. *FASEB J*. 2017;31(7):2996–3006.
47. Li B, et al. Targeted 25-hydroxyvitamin D3 1α-hydroxylase adoptive gene therapy ameliorates dss-induced colitis without causing hypercalcemia in mice. *Mol Ther*. 2015;23(2):339–351.
48. Eming SA, Wynn TA, Martin P. Inflammation and metabolism in tissue repair and regeneration. *Science*. 2017;356(6342):1026–1030.
49. Chen W, et al. PDGFB-based stem cell gene therapy increases bone strength in the mouse. *Proc Natl Acad Sci USA*. 2015;112(29):E3893–E3900.
50. Gregory CA, Gunn WG, Peister A, Prockop DJ. An Alizarin red-based assay of mineralization by adherent cells in culture: comparison with cetylpyridinium chloride extraction. *Anal Biochem*. 2004;329(1):77–84.
51. Wang X, et al. Targeting Non-classical Myelin Epitopes to Treat Experimental Autoimmune Encephalomyelitis. *Sci Rep*. 2016;6:36064.